

AUTOMATIC EVALUATION OF SEGMENTATION METHODS FOR SAR IMAGES

D. C. Zanotta ^{a,b,*}, T. S. Korting ^a, L. M. G. Fonseca ^a, L. V. Dutra ^a

a National Institute for Space Research – INPE CEP - 12245-970 - São José dos Campos - SP, Brazil; {zanotta, tkorting, leila, dutra}@dpi.inpe.br

b Federal Institute for Science, Education and Technology at Rio Grande do Sul – IFRS – Rio Grande – RS, Brazil
daniel.zanotta@riogrande.ifrs.edu.br

KEY WORDS: Image Segmentation, SAR images, Algorithm Evaluation, Empirical Discrepancy Method, Border and Region Measures

ABSTRACT:

This work aims at comparing the performance of different segmentation algorithms in an example of SAR image from Amazonia. The comparison was made by evaluating measures associated with regions and borders of segments obtained by each of the tested optic-specific and SAR-specific segmentation routines. In optic-specific segmentation, some filtering pre-processing was needed to adjust the SAR image to further segmentation. In order to access the accuracy, the segmentations were compared with a reference image through a quantitative evaluation fashion. The results showed by graphs indicate superiority of SAR-specific segmentation performance.

1. INTRODUCTION

Since the last decades, Synthetic Aperture Radar (SAR) images are providing a wealth of images that carry important information on the types of observed surface (Kim et al., 2010). Rather than optical images, SAR images take advantage of collecting data even in cloudy atmospheric situations as well as during night. As in optical images, SAR images require classification to connect image features to different thematic classes. In this sense, object based classification has been increasingly used to classify blocks of pixels instead of individual pixels (Zhou and Troy, 2008). Object based classification proceeds by applying image segmentation followed by region labeling. Performing SAR image segmentation by traditional algorithms developed for optical images (optical-specific) generally presents poor results because the speckle noise present in SAR images, which produces high frequency texture (Saad et al., 1996; Lee, 1986). To circumvent this problem, radar images are often spatially filtered before segmentation step. This process inevitably leads to loss of information. On the other hand, some works have focused on the development of specific algorithms to deal with non-filtered SAR image (SAR-specific), which take into account the Gamma distribution inherent in these images (Zaart et al., 2002).

In this work, we compare the two above mentioned segmentation procedures applied to SAR images from a forest area located in the Amazon rainforest. To evaluate the results, a quantitative approach based on the empirical discrepancy method (Delves et al., 1992) was considered. The aspects taken into account in this evaluation are size, location, average intensity, and shape of segments. The measures are separated into two different characteristics: border and regions (Delves et al., 1992).

2. METHODOLOGY

A large variety of different segmentation algorithms has been proposed for very different concepts and applications. In this work, the following widely-used algorithms were considered: two optical-specific region growing segmentation algorithms proposed (1) by Bins et al. (1996), and (2) by Baatz and Schäpe (2000), both available in the software InterIMAGE (Costa et al., 2010), and SegSAR 1.0 (Sousa, 2005), which stands here for SAR-specific segmentation algorithm. In order to reduce the speckle noise before segmentation by optical-specific algorithms the images were spatially filtered.

The optical-specific algorithm based on Bins et al. (1996) performs an analysis in which each particular segment is formed if two adjacent pixels or regions present a similarity measure satisfying a given threshold. The optical-specific algorithm based on Baatz and Schäpe (2000) is a bottom-up region-merging technique starting in the pixel level. Groups of pixels form smaller objects, and these are successively merged into bigger ones. The SegSAR is a SAR-specific segmentation algorithm which uses region growing, split and merge, and edge adjustment techniques. It considers the SAR statistical properties, such as multiplicative noise propagation and gamma distributed data (Sousa, 2005).

In this work we used two SAR sample test images (Figures 1a and 1c) from Paragominas (PA) – Brazil, acquired in P-band to perform our experiments. Paragominas is located in the north of Brazilian Amazonia. In terms of spatial homogeneity, the first image is more complex whereas the second is quite simple. To run the empirical discrepancy evaluation method, we consider a reference image as segmentation parameter. This image, called phantom image, was manually produced for both test images (Figure 1b and 1d). For each segmentation procedure, many experiments were performed to select the segmentation parameters that produced the most acceptable results.

* Corresponding Author

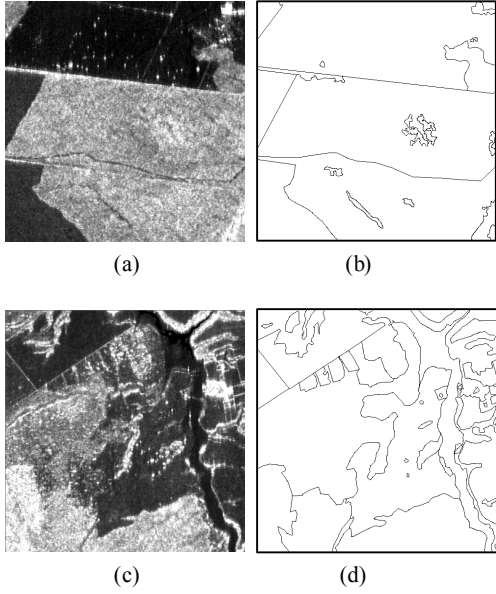


Figure 1. SAR test images: (a) First SAR test image (P-band) and (b) its reference segmentation, (c) Second SAR test image (P-band) and (d) its reference segmentation.

2.1 Region Evaluation

The evaluation of the segmented images can be done in a qualitative or quantitative manner, according to the segmentation used and the concerned application. In this work, the quantitative evaluation using the empirical discrepancy method was investigated. The segmentation quality measure is performed by measuring the size, location, and average intensity of segments.

In order to describe the evaluation method, consider a segmented and an original image, both with x columns and y rows. A region in the reference and in the segmented image is referenced as $1 \leq i \leq N$ and $1 \leq f \leq M$, respectively. Let $\langle g \rangle$ and $\langle g' \rangle$ denote averages of g over a simple sub-region in the reference and segmented image, respectively, and let $N(i)$ and $N(f)$ be the averages of the number of pixels in regions i and f . For two N by M arrays, the indices Goodness of Fit (G) and Fit , are constructed respectively by:

$$G(i, f) = \frac{N(i \cap f)}{N(i \cup f)} \quad (1)$$

$$Fit(i, f) = \frac{x_d + y_d + \frac{P_d + i_d}{2}}{N(i \cup f)}, \quad (2)$$

with

$$x_d = \frac{|\langle x_i \rangle - \langle x_f \rangle|}{x}, \quad y_d = \frac{|\langle y_i \rangle - \langle y_f \rangle|}{y}, \quad (3)$$

$$P_d = \frac{N(i) - N(f)}{N(i) + N(f)}, \quad \text{and} \quad i_d = \frac{|\langle I_i \rangle - \langle I_f \rangle|}{|\langle I_i \rangle + \langle I_f \rangle|},$$

where $\langle x_k \rangle$, $\langle y_k \rangle$, and $\langle I_k \rangle$ are values that correspond respectively to the abscises, ordinates, and gray levels in the k -th region.

The values in the Fit matrix represent a rather heuristic ‘‘average misfit’’ between regions i and f , where the average takes into account region size, location, and intensity. For each I , its corresponding segmented region is considered to have the minimum value of $Fit(i, f)$.

For each shape in the reference image, a number of goodness of fit measures are calculated, each one designed to measure one particular aspect of the fitting process: Goodness of fit for position (Fit_{xy}), Goodness of fit for intensity (Fit_i), Goodness of fit for size (Fit_n) and Goodness of fit for shape (G_{shape}):

$$Fit_{xy} = 1 - \frac{x_d + y_d}{2}$$

$$Fit_i = 1 - \frac{|\langle I_i \rangle - \langle I_f \rangle|}{|\langle I_i \rangle + \langle I_f \rangle|} \quad (4)$$

$$Fit_n = 1 - \frac{N(i) - N(f)}{N(i) + N(f)}$$

$$G_{shape} = \frac{N(i \cap f)}{N(i \cup f)}$$

All measures range continuously from 0 to 1, with 1 being the most desirable value. The Euclidean distance (d_{E2}) in a four-dimension space (R^4), related to the point (1, 1, 1, 1), considers the Fit_{xy} , Fit_i , Fit_n , and G_{shape} measures:

$$d_{E2} = \sqrt{(Fit_{xy} - 1)^2 + (Fit_i - 1)^2 + (Fit_n - 1)^2 + (G_{shape} - 1)^2}, \quad (5)$$

where d_{E2} ranges continuously from 0 to 2. According to this method, since the four values of goodness are subtracted from one in (7), the best segmentation result is the one that produces the smallest d_{E2} . It seeks therefore the best segmentation through the minimization of d_{E2} .

2.2 Border Evaluation

The difference between the detected borders in the reference and segmented images can be calculated through the quantitative assessment of certain measures. The employed border measures accounts for the percentage of correctly detected border pixels (P_{co}), percentage of no detected border pixels (P_{mi}), percentage of wrongly detected border pixels (P_{fa}) and the Pratt figure of merit ($FigMer$). They are computed in the following form:

$$P_{co} = \frac{\text{number of correctly detected border pixels}}{\text{number of reference border pixels}}$$

$$P_{mi} = \frac{\text{number of no detected border pixels}}{\text{number of reference border pixels}}$$

$$P_{fa} = \frac{\text{number of wrongly detected border pixels}}{\text{number of detected border pixels}}$$

$$FigMer = \frac{1}{R} \sum_{i=1}^S \frac{1}{1 + \alpha d(i)^2}, \quad (6)$$

where R and S are number of border reference pixels and border segmented pixels, respectively; α is the scale factor (usually equal to 1); and $d(i)$ is the distance between border pixels found in the reference and segmented images (Scofield et al., 2007).

The measures as described in Equations (8) to (11) vary between 0 to 1, where 1 represents the perfect adjustment for P_{co} and $FigMer$, and 0 the perfect adjustment to P_{mi} and P_{fa} . The Euclidean distance (d_{E2}) in R^4 is used as a global measure of segmentation performance in relation to the detected border quality (Scofield et al., 2007). So, the distance to the point (1,0,0,1) is calculated as:

$$d_{E2} = \sqrt{(P_{co} - 1)^2 + P_{mi}^2 + P_{fa}^2 + (FigMer - 1)^2}, \quad (7)$$

where d_{E2} values range from 0 to 2, with 0 being value for the perfect adjustment of this measure, what implies that the best segmentation will be judged by the minimum distance value.

3. PRELIMINARY RESULTS

The segmented images derived from each tested procedure (filtering + segmentation, or only segmentation in the case of SAR-specific) were evaluated by the empirical discrepancy method. Figure 2 shows segmentation results for both images.

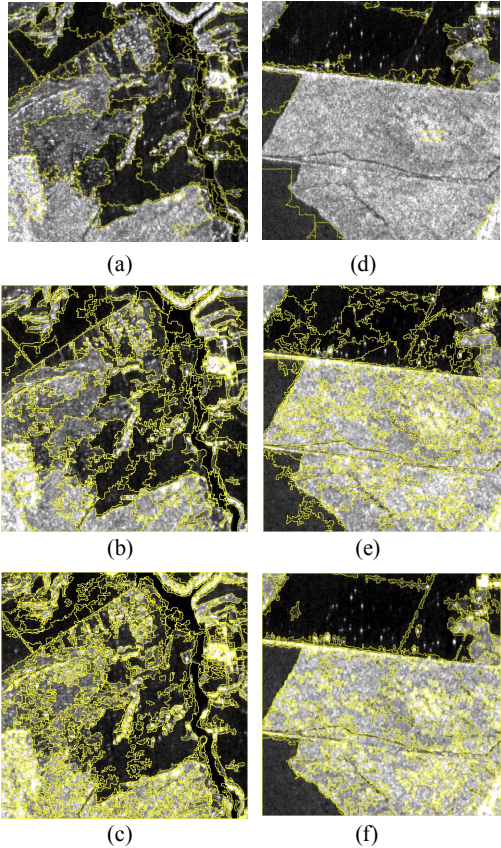


Figure 2. Segmentation results for each tested procedure: (a), (b), and (c) refer to the first test image, whereas (d), (e), and (f) refer to the second one. Segmentation limits appear in yellow.

Figure 3 shows the results for each segmentation method and analyzed parameter. Although we depict all parameters in the diagrams of Figure 3, it is worth stating that the most important one is the Euclidian Distance (d_{E2}), since it combines the parameters of goodness for each characteristic: region and border (Delves et al., 1992). The diagrams show that d_{E2} reaches better value for SegSAR than Baatz and Schäpe (2000) and Bins et al. (1996), in the case of border evaluations (Figure 3a). Among the optical-specific methods analyzed, the algorithm proposed by Baatz and Schäpe (2000) achieves more effective results than the one proposed by Bins et al. (1996).

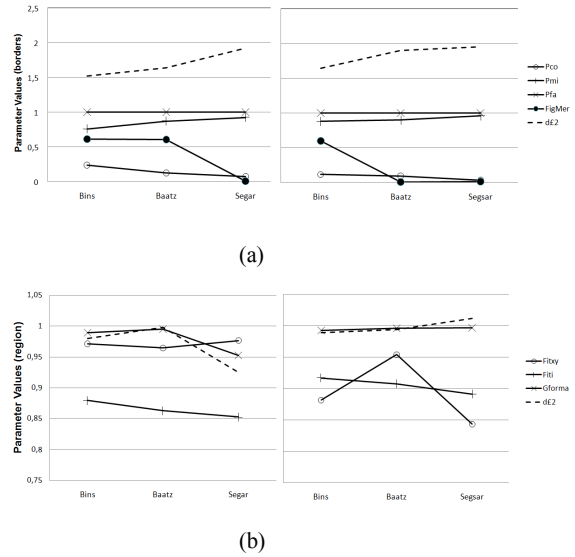


Figure 3. Parameters values considering the borders (a) and region characteristics (b).

For measures based on the region criterion (Figure 3b), d_{E2} also indicate the SegSAR segmentation as the best result for the first test image, although the same was not verified in the second test image. The SegSAR segmentation results for the second test image appears to be controversy once the second test image has low complexity segments and great radiometric differences among regions. Mainly in the second image, it is easy to recognize that SegSAR segmentation results present large regions poorly segmented (some evident limits were not delimited, whereas some homogeneous regions were). This can be explained by the SegSAR segmentation principle, which considers a Gamma statistical distribution in the cartoon model. On the other hand, this explanation could be the major reason for the better performance of SegSAR algorithm in relation to the optical-specific segmentation algorithms.

4. CONCLUSIONS

This work aimed to test two different segmentation principles in a set of P-band SAR images. The segmentation procedures tested were: (1) filtering followed by segmentation in an optical-specific perspective, and (2) direct segmentation performed by SAR-specific segmentation algorithm. The evaluation was carried out by means of region and borders characteristics of segments, according to the empirical

discrepancy method. The preliminary results confirm the relative advantage of SAR-specific segmentation algorithm over optical-specific ones applied to SAR images. Nevertheless, experiments with more types of SAR-specific and optical-specific methods as well as test images are required to overall conclusions.

5. REFERENCES

- Baatz, M., Schäpe, A., 2000. Multiresolution segmentation: an optimization approach for high quality multi-scale image segmentation. *XII Angewandte Geographische Informationsverarbeitung*, Wichmann Verlag, Heidelberg.
- Bins, L.S., Fonseca, L.M.G., Erthal, G.J., Li, F.M., 1996. Satellite imagery segmentation: a region growing approach. *VIII Simpósio Brasileiro de Sensoriamento Remoto*, Salvador, BA. pp. 677-680.
- Costa, G.A.O.P., Feitosa, R.Q., Fonseca, L.M.G., Oliveira, D.A.B., Ferreira, R.S., Castejon, E.F., 2010. Knowledge-based interpretation of remote sensing data with the interimage system: major characteristics and recent developments. *GEOBIA*. Gent, Belgium.
- Delves, L. M., Wilkinson, R., Oliver, C. J., White, R. G., 1992. Comparing the performance of SAR segmentation algorithms. *International Journal of Remote Sensing*, 13(11), pp. 2121—2149.
- Kim, D. Jin, Moon, W. M., Kim, Y. Soo., 2010. Application of Terra SAR-X data for emergent Oil-Spill monitoring. *Ratio*, 48(2), pp. 852-863.
- Lee, J.S., 1986. Speckle suppression and analysis for SAR images, *Optical Engineering*. 25(5), pp. 636–643.
- Saad, A., El Assad, S., Barba, D., 1996. Speckle filtering in SAR images by contrast modification, comparison with a large class of filters, *Ann. TelTelecommun.* 51(5–6), pp. 233–244.
- Scofield, G. B.; Santanna, S. J. S.; Freitas, C. C.; Dutra, L. V. Avaliação quantitativa do SegSAR através de medidas de borda e regiões em imagens ópticas sintéticas. In: simpósio brasileiro de sensoriamento remoto, 13. (SBSR), 2007, Florianópolis. Anais... São José dos Campos: INPE, 2007. p. 6167-6174. CD-ROM; On-line. ISBN 978-85-17-00031-7.
- Sousa Jr, M. A., 2005. Segmentação multi-níveis e multi-modelos para imagens de radar e ópticas. 133 p. Tese (Doutorado em Computação Aplicada) - Instituto Nacional de Pesquisas Espaciais, São José dos Campos.
- Zaart, E., Ziou, D., Wang, S., Jiang, Q., 2002. Segmentation of SAR images, *Pattern Recognition*, 35 (3), pp. 713-724.
- Zhou, W., Troy, A., 2008. An object-oriented approach for analyzing and characterizing urban landscape at the parcel level. *International Journal of Remote Sensing*, 29(11), pp. 3119—3135.